Published in final edited form as:
J Phys Chem A. 2009 October 22; 113(42): 11262–11265. doi:10.1021/jp906188k.

Rotational Structure of a Super-Excited State of the NO Molecule Revealed by OODR-Multiphoton Laser Spectroscopy

Yong-Ge Lin, **Jorge E. Colón-García**, **Carlos R. Cabrera**, and **Edwin Quiñones***
Department of Chemistry, University of Puerto Rico, Río Piedras Campus, P.O. Box 23346, San Juan, Puerto Rico 00931

Abstract

The optical–optical double resonance time of flight (OODR-TOF) spectroscopy technique was employed to examine the 65 000–66 500 cm^{-1} region of the nitric oxide spectrum. In this region, we detected the following three electronic states: E $^2\Sigma^+$ (v = 2) (Rydberg state), B $^2\Pi$ (v = 23) (valence state), and L $^2\Pi$ (v = 4) (valence state). The rotational structure analysis of an unexpected band in the red part of the spectra revealed the presence of a new super-excited $^2\Sigma^+$ Rydberg state at ~13.3 eV, which was populated through a three-photon transition from the intermediate A $^2\Sigma^+$ (v = 0) state. This super-excited state converges to the NO ($a^3\Sigma^+$) ionic state with electronic configuration $(1\sigma)^2(2\sigma)^2(3\sigma)^2(4\sigma)^2(5\sigma)^2(1\pi)^3(2\pi)^1(3s\sigma)^1$.

1. Introduction

The implementation of optical–optical double resonance schemes has led to an enormous simplification of molecular spectra and may facilitate one to reach Franck–Condon regions not accessible from the ground state and to drive multiphoton transitions.[1–9] The implementation of mass detection opened up the prospects of studying excited states that lie in the vacuum ultraviolet region, thereby overcoming the problem of light absorption by air. In this work, we report a new electronic state of NO that lies at 13.3 eV, taking advantage of the features mentioned. This state is located in the region of the so-called “super-excited states” that have been studied using high-order laser harmonics or synchrotron radiation.[10–13] Computational studies have also been done in this region to understand the photoionization processes.[14,15] The new state was reached by first pumping individual rotational levels of the intermediate A $^2\Sigma^+$ (v = 0) state, and then scanning a dye laser in the visible region to drive a three-photon transition. In the same OODR-TOF spectra also appear the following states: E $^2\Sigma^+$ (v = 2) (Rydberg state), B $^2\Pi$ (v = 23) (valence states), and L $^2\Pi$ (v = 4) (valence states). These states lie at ~6.3 eV and are reached through one-photon absorption from the intermediate state. The excitation scheme is similar to that of Ishiwata et al., who recorded OODR spectra of Br_2 using a two-photon transition from the intermediate state to reach a new ion-pair state.[16] We deduced that this is a Rydberg $^2\Sigma^+$ state through a rotational analysis, which has been considered to be the most reliable tool to assign the term symbol of an electronic state. Nevertheless, because the information about rotational structures has been missing in studies that involve the one-photon excitation process with the synchrotron radiation as the excitation source, the super-excited Rydberg states at energies above 13 eV were usually assigned by using the quantum defect analysis.[11,12]

* Corresponding author. Tel.: (787) 764-0000, ext. 4810. equinones@uprrp.edu..

2. Experimental Section

The instrumental setup employed in this work has been described elsewhere.17¯19 Commercial nitric oxide (99.5%, AGA Products) mixed with argon was expanded into the source chamber using a pulsed-nozzle valve. The NO/Ar gas pulse was skimmed before it entered the detection chamber. The molecular beam direction was perpendicular to the propagation direction of the two laser beams. The pressure in the detection chamber was below 1×10^{-4} Torr when the pulsed nozzle valve was operating. Individual rotational states of the A electronic state of NO were excited using an excimer-pumped dye laser, equipped with a BBOI doubling crystal. The beam was focused onto an area of ~1 mm^2 using a cylindrical lens (focal length 100 cm). A tunable dye laser (Scanmate, Lambda Physik) pumped by a Nd:YAG laser (LPY 150, Lambda Physik) was used to carry out the second resonance as well as to ionize the highly excited molecules. The delay time between the two laser pulses was adjusted to 50 ns using a digital pulse generator. The NO^+ ion signal was detected by a homemade Wiley–McLaren linear time-of-flight spectrometer (TOF) system with a flight distance of a half meter.17,19

3. Results and Discussion

In the present Article, we report the observation of a new excited state at 13.3 eV of nitric oxide, which lies at 4 eV above the onset of the first ionization continuum. The detection of this so-called super-excited state was achieved using two tunable dye lasers. The first laser pulse (UV light, ~4 eV) prepared individual rotational levels of the intermediate A $^2\Sigma^+$ (v = 0) state of NO, denoted from now on as the intermediate state. The second laser (visible light, ~2.6 eV) excited two types of transitions: (i) a one-photon transition to reach electronic states of NO below the first ionization continuum, and (ii) a three-photon transition to reach the excited state above the onset of the first ionization continuum. Although quite different energies are involved, both types of transitions appear in the same spectral region. We first present an analysis of the states observed through the one-photon process because the information generated facilitated the analysis of the “super-excited” states.

3.1. States Below the First Ionization Continuum

In Figure 2 are observed the following three electronic states: E $^2\Sigma^+$ (v = 2) (Rydberg state), B $^2\Pi$ (v = 23) (valence state), and L $^2\Pi$ (v = 4) (valence state). These states are reached through a one-photon transition driven by the second laser, using the A state as a stepping stone. The relative position of these states as a function of rotational quantum number is presented in Figure 1, which was constructed using the molecular constants listed in Table 1. For each rotational level of the NO intermediate state, the spectra display the following eight lines for the B–A (23, 0) band: $^{O}P^{f}_{12}$, P^{e}_{11}, Q^{f}_{11}, R^{e}_{11}, P^{f}_{22}, P^{e}_{21}, Q^{f}_{21}, and $^{S}R^{e}_{21}$ (from left to right). While the L–A (4, 0) band should also present eight lines, some are missing, and the same observation has been made by other authors.20 Above J = 13.5, the B–A (23, 0) transitions become extremely weak and are no longer observed. An energy against the $N(N + 1)$ plot for the E–A (2,0) band exhibits a linear behavior from N = 0 to N = 20, as shown in Figure 3. This means that the E_2 state is not perturbed. Because both the E and the A states are Rydberg states and belong to Hund's case (b), the E–A (2, 0) band consists of only two lines. The line positions of the E–A (2, 0) and B–A (23, 0) bands have been compiled in Tables 2 and 3, respectively.

3.2. States Above the First Ionization Continuum

Besides the three bands previously discussed, the spectra exhibit a hitherto unassigned band that consists of two lines located in the left part of the spectra of Figure 2. The observation

of only two transitions in each spectrum is characteristic of a $^2\Sigma^+$–$^2\Sigma^+$ transition. The midpoint between the P and R lines maintains a constant separation from the E–A (2, 0) band, as expected for a Rydberg $^2\Sigma^+$ state. However, what it is peculiar of this band is that the separation between the P and R lines is one-third of the corresponding separation on the E–A (2, 0) band. This difference may be explained postulating a three-photon absorption process from the A state, as illustrated in Figure 4. The following arguments support this assignment. First, the selection rule for one-photon and three-photon transitions is essentially the same, which means that the pattern of the new band is similar to that of the E–A band.16,21,22 In Table 4 are listed the energies of the rotational states reached. Second, we can discard the absorption of three photons from the ground state to reach a state around 7.5 eV because otherwise we should be detecting numerous lines corresponding to the rotational states thermally populated in the ground state. Third, the ground state has $^2\Pi$ symmetry, and the band observed clearly corresponds to a $^2\Sigma^+$–$^2\Sigma^+$ transition. Forth, from the *E* versus $N(N + 1)$ curve in Figure 5, we derived the rotational constant to be 2.00 cm^{-1}, which agrees with the value expected for a Rydberg state. The term value of this state is 106 735 (~13.3 eV), which is ~4eV above the threshold of the first ionization continuum (~9.26 eV). This term value belongs to one of those super-excited states that have recently been investigated exciting NO (with the photon energies of 9–35 eV) using high-order harmonic laser or synchrotron lights.11,12,23–27 The nearby super-excited Rydberg $^2\Sigma^+$ state with the extremely sharp intense line, located at the energy of 13.818 eV, has been observed with the angle-resolved constant-ionic-state (CIS) technique, using one-photon excitation from the ground state.12,27 Salzmann et al. reported that the autoionization via this resonant Rydberg excitation leads to a 10-fold increase of the ionization cross section.27 This enhanced autoionization mechanism may explain why we can observe ion signal from this new Rydberg $^2\Sigma^+$ state. While the assignment of the symmetry of the super-excited states of NO has usually been done using the quantum defect theory, an assignment based on a rotational structures analysis, as has been presented in Figure 5, is more definitive.11

3.3. Electronic Configuration of the New State

The electronic configuration for this new super-excited state may be assigned with the aid of existing theoretical and experimental results.12–15,27 The electronic configuration for the NO ground state ($X^2\Pi$) is usually represented as $(1\sigma)^2(2\sigma)^2(3\sigma)^2(4\sigma)^2(5\sigma)^2\text{-}(1\pi)^4(2\pi)^1$. The removal of one electron from the (2π), (1π), and (5σ) orbitals gives rise the lowest three ionic states: $X^1\Sigma^+$, $a^3\Sigma^+$, and $b^3\Pi$ states, with ionization energies of 9.26, 15.67, and 16.56 eV, respectively. The potential energy curves for the NO neutral ground state and the ionic states may be found in the literature.27,28 The nomenclature of the term symbols used to describe the NO super-excited states is different from that used for the excited states. A series of neutral super-excited states will be called $b^3\Pi$ or $a^3\Sigma^+$ series if they converge to the NO^+ ($b^3\Pi$) or NO^+ ($a^3\Sigma^+$) ionic state. The states are described by providing information of the converging ionic state and information of the highest occupied electron: NO (converging ionic state, highest occupied orbital). As far as the neutral states of overall $^2\Sigma^+$ symmetry above 13 eV are concerned, we need to note that the $(2\pi)^{-1}$ ionization via the 2π–kσ transition only gives rise to a continuum shape resonance centered at 14 eV. Although both NO ($b^3\Pi$, npπ) series and NO ($a^3\Sigma^+$, nsσ) series include $^2\Sigma^+$ states, our newfound $^2\Sigma^+$ state should belong to the $a^3\Sigma^+$ Rydberg series for energetic reasons. That is to say, the lowest member of the NO ($b^3\Pi$, 3p) series of Rydberg states has an energy of 13.818 eV (or possibly as low as 13.654 eV), whereas the state we observed lies at 13.3 eV.12,14,15,27 In addition, theory predicts that the NO ($a^3\Sigma^+$, nsσ) series should have members with $^2\Sigma^+$ symmetry in the region between 12.61 and 15.06 eV,15 and experimentally the NO ($a^3\Sigma^+$, 4sσ)–NO ($X^2\Pi$) transition bands have been observed between 14.1 and 15.2 eV.12 It follows that the new state can only be a resonant state of NO ($a^3\Sigma^+$, 3sσ), which has the following electronic configuration: $(1\sigma)^2(2\sigma)^2(3\sigma)^2(4\sigma)^2(5\sigma)^2(1\pi)^3(2\pi)^1(3s\sigma)^1$.

Acknowledgments

This work was supported by the NIH-SCoRE Program and by the NASA-UPR Center for Advanced Nanoscale Materials funded through the NASA Space Grant.

References and Notes

1. Cheung WY, Chupka WA, Colson SD, Gauyacq D, Avouris P, Wynne JJ. J. Chem. Phys. 1983; 78:3625.
2. Seaver M, Chupka WA, Colson SD, Gauyacq D. J. Phys. Chem. 1983; 87:2226.
3. Ebata T, Mikami N, Ito M. J. Chem. Phys. 1983; 78:1132.
4. Zhao RC, Konen IM, Zare RN. J. Chem. Phys. 2004; 121:9938. [PubMed: 15549868]
5. Cheung WY, Chupka WA, Colson SD, Gauyacq D, Avouris P, Wynne JJ. J. Phys. Chem. 1986; 90:1086.
6. Biernacki D, Colson S, Eyler EE. J. Chem. Phys. 1988; 88:2099.
7. Ebata T, Anezaki Y, Fujii M, Mikami N, Ito M. J. Phys. Chem. 1983; 87:4773.
8. Achiba Y, Sato K, Shobatake K, Kimura K. J. Chem. Phys. 1983; 78:54745479.
9. Sirkin ER, Asscher M, Haas Y. Chem. Phys. Lett. 1982; 86:265.
10. Alvarez Ruiz, J. Photon Induced Fluorescence Studies of Molecules Using Synchrotron Radiation. Stockholm; KTH, Physics: 2003.
11. Ehresmann A, Liebel H, Von Kroger M, Schmoranzer H. J. Phys. B: At. Mol. Opt. Phys. 2001; 34:2893.
12. Innocenti F, Costa ML, Dias AA, Goubet M, Morris A, Oleriu RI, Stranges S, Zema N. Mol. Phys. 2007; 105:771.
13. Southworth SH, Parr AC, Hardis JE, Dehmer JL. J. Chem. Phys. 1987; 87:5125.
14. Stratmann RE, Zurales RW, Lucchese RR. J. Chem. Phys. 1996; 104:8989.
15. Lynch DL, Schneider BI, Collins LA. Phys. Rev. A. 1988; 38:4927. [PubMed: 9900974]
16. Ishiwata T, Tokunaga A, Shinzawa T, Tanaka I. Bull. Chem. Soc. Jpn. 1984; 57:1469.
17. Conde C, Maul C, Quinones E. J. Phys. Chem. A. 1999; 103:1929.
18. Lei, Y. Ph.D. Thesis. University of Puerto Rico; San Juan: 2003. Mechanism of the Multiphoton Dissociation of SO_2 via the H Rydberg State and Laser Initiated Processes within $(SO_2)_m(NO)_n$ Van Der Waals Clusters..
19. Dixit AA, Lei Y, Lee KW, Quinones E, Houston PL. J. Phys. Chem. A. 2005; 109:1770. [PubMed: 16833505]
20. Dressler K, Miescher E. J. Chem. Phys. 1981; 75:4310.
21. He J, Scholes GD, Ang YL, Ji W, Beh CWJ, Chin WS. Appl. Phys. Lett. 2008; 92:131114.
22. Xie, X.-b.; Wang, P-Q.; Cao, C-S.; Sun, T-H. Chin. Phys. Lett. 1999; 16:816.
23. Erman P, Karawajczyk A, Rachlew-Kallne E, Stankiewicz M, Yoshiki Franzen K, Sannes P, Veseth L. Chem. Phys. Lett. 1997; 273:239.
24. Mitsuke K, Hikosaka Y, Hikida T, Hattori H. J. Electron Spectrosc. Relat. Phenom. 1996; 79:395.
25. Erman P, Karawajczyk A, Rachlew-Kallne E, Mevel E, Zerne R, L'Huillier A, Wahlstrom CG. Chem. Phys. Lett. 1995; 239:6.
26. Ehresmann A, Liebel H, Von Kroger M, Schmoranzer H. J. Phys. B: At. Mol. Opt. Phys. 2001; 34:3119.
27. Salzmann M, Muller M, Bowering N, Heinzmann U. J. Phys. B: At. Mol. Opt. Phys. 1999; 32:2517.
28. Albritton DL, Schmeltekopf AL, Zare RN. J. Chem. Phys. 1979; 71:3271.

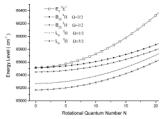

Figure 1.
Energy versus *N* plots constructed with the molecular constants from the literature listed in Table 1.

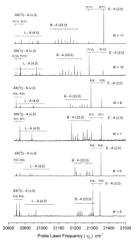

Figure 2.
Representative spectra in which the E_2 and B_{23} states are detected. The marked line positions for the B–A (23, 0) band are assigned as as $^{O}P^{f}_{12}$, P^{e}_{11}, Q^{f}_{11}, R^{e}_{11}, P^{f}_{22}, P^{e}_{21}, Q^{f}_{21}, and $^{S}R^{e}_{21}$, from left to right.

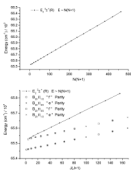

Figure 3.
Rotational energy levels for the E_2 and B_{23} states. Lower part: $E \approx J(J + 1)$ relations for F_1 and F_2 of the B_{23} state specifying e and f symmetry in rotational levels below $J = 12$. Upper part: $E \approx N(N + 1)$ relation for the E_2 state including rotational levels up to $N = 20$.

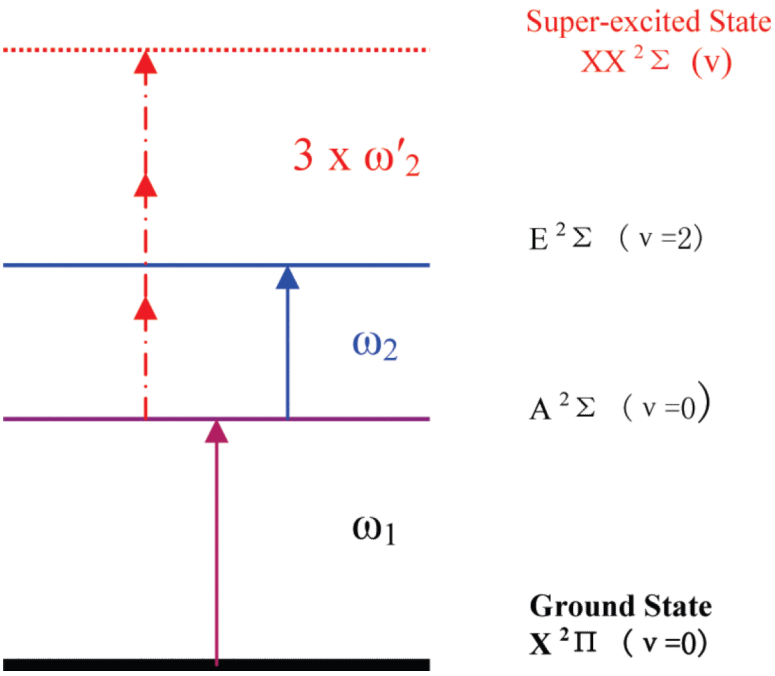

Figure 4.
Diagram of the XX–A band mechanism.

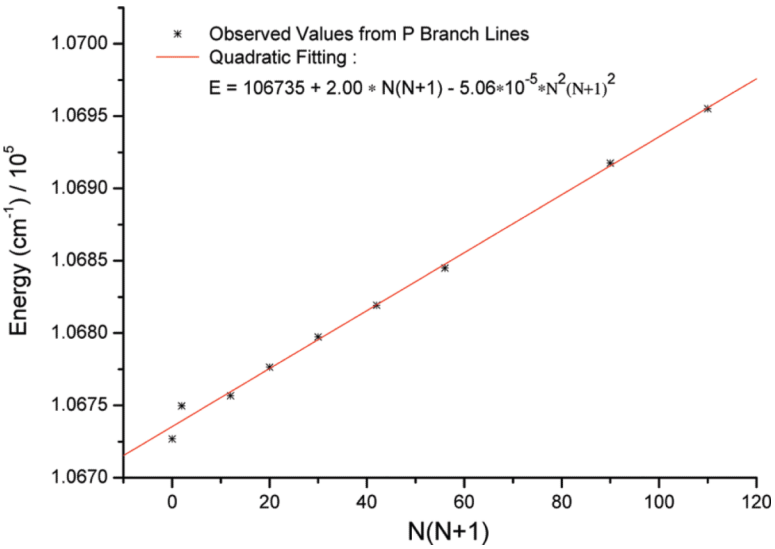

Figure 5.
Rotational energy levels of the XX state.

TABLE 1

Molecular Constant Summary for NO Electronic States[a]

term	*v*	T_v	ω_e	$\omega_e\chi_e$	B_v	D_e	α_e
x $^2\Pi_{3/2}{}^*$ (a)	0	0	1904	14.1	1.663	0.54×10^{-6}	0.0171
X $^2\Pi_{1/2}{}^*$ (a)	0	0	1904	14.1	1.711	10.2×10^{-6}	0.0182
A $^2\Sigma^+$ (c)	0	44 200	2374	16.1	1.989	4.6×10^{-6} (a)	0.0187
l $^2\Pi_{3/2}$ (g)	4^*	64 300	974.6	11.3	1.055		0.0220
l $^2\Pi_{1/2}$ (g)	4^*	64 390	974.6	11.3	1.055		0.0220
B $^2\Pi_{3/2}$ (a)	23	65 517	1040	8.3	0.85	4.9×10^{-6}	0.0120
B $^2\Pi_{1/2}$ (a)	23	65 448	1037	7.7	0.82	4.9×10^{-6}	0.0120
E $^2\Sigma^+$ (i)	2	65 515	2375	16.4	1.941	5.6×10^{-6}	0.0182

[a] T_V is the total energy (cm^{-1}) of level $N = 0$, relative to X $^2\Pi$ ($v = 0$, $J = 1/2$). The following constants are in cm^{-1}: ω_e, $\omega_e\chi_e$, B_e, B_v, and D_e. The reference remarks on specific data override the remarks on terms. The description of items marked with the sign

* is as follows: L ($v = 4$) was previously classified as L ($v = 3$). For the ground state X $^2\Pi$, the calculation of the rotational energy required the *Y* constant, whose value (72.61942) was obtained treating this state as an intermediate between Hund's case (a) and (b). The reference marks refer to the following literature: (a) NIST Web Book; (b) Conde et al. (1998); (c) Brunger et al. (2000); (g) Dressler and Miescher (1981); (i) Dressler (1965).

TABLE 2

Observed E–A (2, 0) Band Lines[a]

intermediate A $^2\Sigma^+$ (v = 0)		target E $^2\Sigma^+$ (v = 2)	
N'	energy (cm^{-1})	P lines ω_2 (cm^{-1})	R lines ω_2 (cm^{-1})
0	44 199.7	–	21 330
1	44 203.6	21 323	21 331
2	44 211.6	21 318	21 337
3	44 223.5	21 315	21 342
4	44 239.4	21 309	21 344
5	44 259.3	21 305	21 348
6	44 283.2	21 301	21 352
7	44 311.0	21 296	21 354
8	44 342.8	21 292	21 359
9	44 378.6	–	–
10	44 418.3	21 283	21 364
11	44 462.1	21 279	21 368
12	44 509.8	21 273	21 370
13	44 561.4	21 269	21 374
14	44 617.1	21 263	21 377
15	44 676.7	21 258	21 377
16	44 740.2	21 253	21 381
17	44 807.7	21 247	21 382
18	44 879.2	–	21 385
19	44 954.7	21 236	21 388
20	45 034.1	21 230	21 395

[a]The mark "–" indicates the missing lines. For the energy calculation, the wavenumber ω_2 shall be calibrated with a factor of 0.999475. The absolute term values of the observed lines can be calculated by the summation of their wavenumbers and the corresponding energy of the related rotational levels in the intermediate A state.

TABLE 3

Observed Lines of B–A (23, 0) Bands[a]

N'	$^{O}P^{f}_{12}$	P^{e}_{11}	Q^{f}_{11}	R^{e}_{11}	P^{f}_{22}	P^{e}_{21}	Q^{f}_{21}	$^{s}R^{e}_{21}$
0	–	–	21 259	21 262	–	–	–	–
1	–	–	21 258	21 263	–	–	21 323	21 331
2	–	21 249	21 254	21 259	–	–	21 322	21 328
3	21 239	21 243	21 249	21 256	21 307	21 311	21 317	21 325
4	21 226	21 231	21 239	21 248	21 293	21 300	21 308	21 317
5	21 211	21 218	21 228	21 239	21 280	21 287	21 296	21 308
6	21 197	21 205	21 215	21 229	21 265	21 275	21 285	21 298
7	21 277	21 187	21 200	21 214	21 245	21 256	21 270	21 284
8	21 157	21 169	21 184	21 199	21 226	21 239	21 254	21 270
10	21 108	21 124	21 141	21 160	21 178	21 195	21 212	21 232
11	21 081	21 098	21 118	21 139	21 151	21 169	21 189	21 210

[a]The “e” and “f” symmetry marks on the first row represent the case in the final states. The mark “–” indicates the missing peaks. For the energy calculation, the wavenumber ω_2 shall be calibrated with a factor of 0.999475. The absolute term values of the observed peaks can be calculated by the summation of their wavenumbers and the corresponding energy of the related rotational levels of the intermediate A state, listed in Table 2.

TABLE 4

Energy Level Accessed by the Three-Photon XX–A(v, 0) Transition Process[a]

intermediate A $^2\Sigma^+$		P lines frequency ω_2 (cm^{-1})	R lines frequency ω_2 (cm^{-1})	P line destination E $E_A + 3\omega_2$*0.999475	R line destination E $E_A + 3\omega_2$*0.999475
N'	energy E_A				
0	44 199.7		20 857		106 737.8
1	44 203.6	20 852	20 857	106 726.8	106 741.8
3	44 223.5	20 853	20 866	106 749.7	106 788.6
4	44 239.4	20 850	20 867	106 756.6	106 807.6
5	44 259.3	20 850	20 865	106 776.5	106 821.4
6	44 283.2	20 849	20 869	106 797.3	106 857.3
7	44 311.0	20 847	20 868	106 819.2	106 882.1
8	44 342.8	20 845	20 871	106 845.0	106 922.9
10	44 418.3	20 844	20 872	106 917.5	107 001.5
11	44 462.1	20 842	20 876	106 955.2	107 057.2
12	44 509.8	20 839	20 876	106 993.9	107 104.9
13	44 561.4	20 839	20 879	107 045.6	107 165.5
14	44 617.1	20 838		107 098.2	

[a]For the energy calculation, the wavenumber ω_2 shall be calibrated with a factor of 0.999475.